

# *Supporting information for*

## **Imaging groundwater infiltration dynamics in karst vadose zone with long-term ERT monitoring**

Arnaud Watlet<sup>1,2</sup>, Olivier Kaufmann<sup>1</sup>, Antoine Triantafyllou<sup>1,3</sup>, Amaël Poulain<sup>4</sup>, Jonathan E. Chambers<sup>5</sup>, Philip I. Meldrum<sup>5</sup>, Paul B. Wilkinson<sup>5</sup>, Vincent Hallet<sup>4</sup>, Yves Quinif<sup>1</sup>, Michel Van Ruymbeke<sup>2</sup>, Michel Van Camp<sup>2</sup>

<sup>1</sup>Geology and Applied Geology Unit, Faculty of Engineering, University of Mons, Place du Parc 20, 7000 Mons, Belgium.

<sup>2</sup>Seismology-Gravimetry, Royal Observatory of Belgium, Avenue Circulaire 3, 1180 Uccle, Belgium.

<sup>3</sup>Laboratoire de Planétologie et Géodynamique — Nantes (LPGN), UFR Sciences et Techniques, Université de Nantes, UMR-CNRS 6112, Rue de la Houssinière 2, BP92208, 44322 Nantes Cedex 3, France

<sup>4</sup>Department of Geology, University of Namur, Rue de Bruxelles 61, 5000 Namur Belgium

<sup>5</sup>Geophysical Tomography Team, British Geological Survey, Nottingham NG12 5GG, UK

Correspondence to: Arnaud Watlet ([arnaud.watlet@umons.ac.be](mailto:arnaud.watlet@umons.ac.be))

### **S1 Temperature correction**

Temperature variations of the subsurface can have significant impacts on resistivity data (Brunet et al., 2010). A vertical profile of temperature sensors (Campbell Instruments) is installed next to the ERT profile for monitoring seasonal temperature variation. As a marked temperature gradient is expected in the sinkhole, an additional network of temperature sensors is installed at 5 cm depth along the surface profile to correct for local temperature variations. Air temperature is also recorded.

Figure 4-10 shows that the temperature data are quite similar along the profile in winter but the distribution becomes widespread in summer. While air mixing is efficient in winter, helped by “warm” air currents coming from the cave in the bottom of the sinkhole, a stratification is observed in summer with cold air trapped in the bottom of the sinkhole. This type of seasonal variations in cave entrances is well-known and has already been by Trombe (1952) in similar environments.

The heat equation characterises temperature variations in a given space. In our case, as temperature variations in the subsurface are mainly affected by changes in air temperature and insulation, internal heating source can be neglected; this relationship can thus be described as follow:

$$\frac{\partial T}{\partial t} = \alpha \nabla^2 T \quad (S1)$$

where  $T$  is the temperature,  $t$  is the time, and  $\alpha$  is the thermal diffusivity of the medium, that relates as:

$$\alpha = \frac{\lambda}{\rho C_p} \quad (S2)$$

In which  $\lambda$  is the thermal conductivity,  $\rho$  the bulk rock density and  $C_p$  the specific heat capacity. Simple models exist to solve Eq. (S1) in the 1D domain and estimate temperature at depth. Amongst them, the approach of Nofziger (2005) is the most commonly used in ERT monitoring experiments (e.g. Brunet et al., 2010; Chambers et al., 2014; Samouëlian et al., 2005; Uhlemann et al., 2016). It approximates the annual ground temperature changes as the sinusoidal function of Hillel (1982) with phase lags in depth given a particular damping depth. However, it assumes that no lateral temperature variation affects the study site, which is true for most case studies. It also leaves uncorrected the resistivity variations from non-seasonal temperature changes.

Given the widespread distribution of temperatures recorded along the ERT profile, especially in summer, we developed a temperature correction approach based on the computation of the 2D temperature field in the vertical plane including the ERT profile. The heat equation Eq. (S1) was solved with the finite elements method using the Crank-Nicolson approximation. We took advantage of the finite elements framework of the Geophysical Inversion and Modelling Library (GIMLi) and its Python environment pyGIMLi (Rücker et al., 2017; [www.pygimli.org](http://www.pygimli.org)) to solve this problem. This provides an environment in line with the resistivity data processing, as the ERT inversion software BERT (Günther et al., 2006; Rücker et al., 2006), used for this study, is also based on GIMLi libraries, while their respective Python wrappers have been developed to be efficiently compatible.

With this finite element approach of the ground heat problem, the boundary conditions and material properties still need to be set. A mesh representing the monitoring profile was built with a large surrounding box of 100 m deep and 200 m of lateral extensions. Neumann boundary conditions are fixed for both lateral boundaries. A fixed Dirichlet boundary conditions is set to the mean annual air temperature (9.3°C) at the bottom limit. The upper limit is defined by variable Dirichlet conditions as a function of the temperature recorded along the ERT profile. To account for the lateral temperature distribution, a series of 1-meter long boundaries are implemented along the topography of the ERT profile. The value of each boundary is determined following an inverse distance weighted (IDW) interpolation of the measured temperature of the sensor network.

**Table S 1 : Properties used to compute the temperature field following Eq. (S1) using Eq. (S2). Parameters of the clay-rich upper layer are chosen as to be the best fit of temperature measurements in the vertical profile (see Fig. S2), whereas those of the limestone lower layer are set from the literature.**

	$\lambda$ (W.m <sup>-1</sup> .K <sup>-1</sup> )	P (kg/m <sup>3</sup> )	Cp (J.kg <sup>-1</sup> .K <sup>-1</sup> )	$\alpha$ (m <sup>2</sup> /s)
Clay-rich upper layer	0.8	1400	1100	5.2
Limestone lower layer	2.8	2800	2200	4.5

Two layers are modelled in the mesh: a thin clay-rich soil layer at surface over a thick limestone layer. Values for the thermal conductivity, density and heat capacity of the limestone layer are set from the literature (Clauser and Huenges, 1995; Vosteen and Schellschmidt, 2003) whereas that of the clay-rich soil layer are fitted from data of the vertical profile of temperature sensors. Chosen values and calculated thermal diffusivity (following Eq. (S2)) are detailed in Table 1. Note that here, we neglect the fact that the thermal properties varies as a function of the moisture content, as evidenced by Farouki (1981). Figure S2 compares the measured temperatures in the vertical profile and markers of the modelled temperature field at the same locations.

Correcting for the effect of temperature in time-lapse ERT can be implemented in several ways. We chose to apply the method described in Hayley (2007) in which the correction of a measured resistivity dataset ( $d_{obs}$ ) is done after correcting the inverted model  $m_{est}$  and subtracting the model response ( $d_{est}$ ) to the resulting corrected model response ( $d_{est}^{TC}$ ), such as:

$$d_{obs}^{TC} = d_{obs} + (d_{est}^{TC} - d_{est}) \quad (S3)$$

The resulting data vector  $d_{obs}^{TC}$  can thus be inverted to produce a resistivity model  $m_{est}^{TC}$  corrected for temperature effects. While this method is time costly because it implies two inversions of the same resistivity dataset, it has the strength of applying an integrated correction on both the apparent and effective resistivity distribution.

The linear model of Keller and Frischknecht (1966) valid between 0 and 25°C, is used to correct the resistivity model  $d_{est}$ . It defines as:

$$\rho_{corr} = \rho_T(1 + m(T - T_{corr})) \quad (S4)$$

where  $\rho_{corr}$  denotes the electrical resistivity corrected at a standard  $T_{corr}$  set in our case to 9.3 °C. A Keller and Frischknecht's coefficient  $m = 0.025 \text{ } ^\circ\text{C}^{-1}$  (Brunet et al., 2010) was fixed as an average estimate of the  $m$  coefficients distribution.

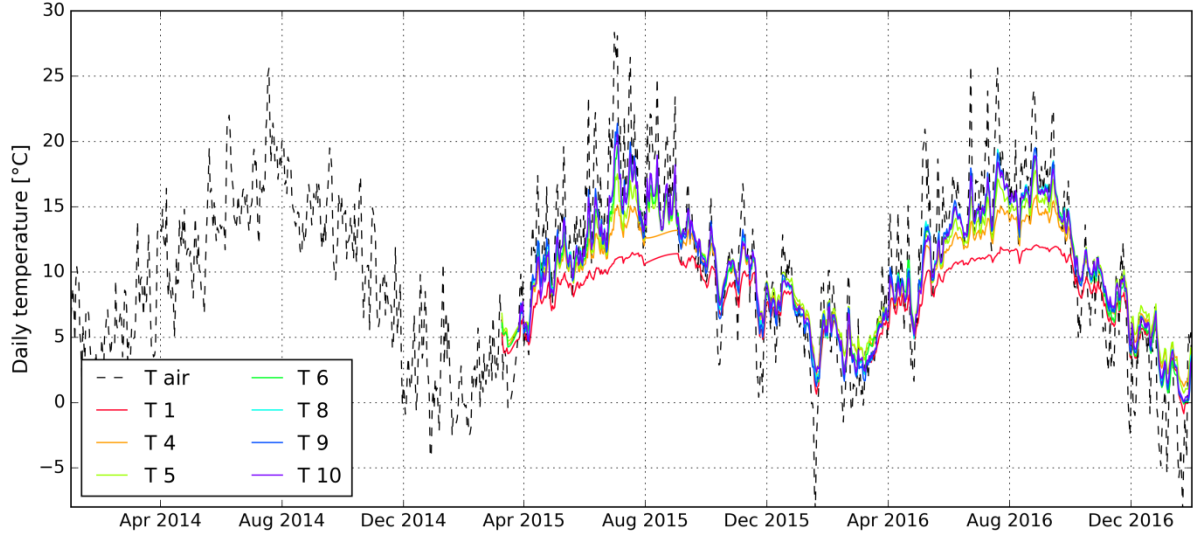


**Figure S1: Temperature monitoring along the ERT profile. The locations of the probes are reported in Figure 4-2.**

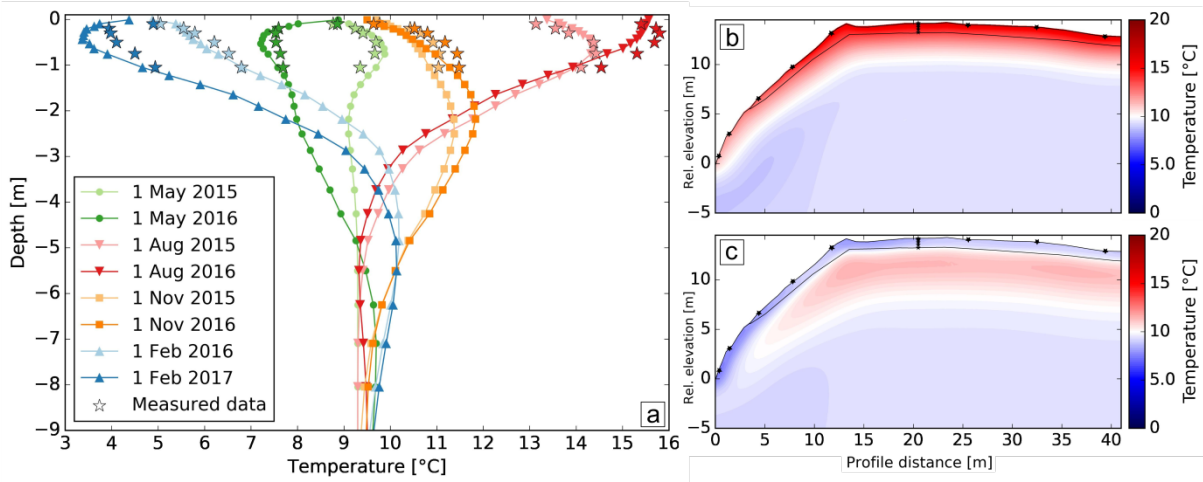


**Figure S2: (a) Measured temperatures in the vertical profile at 8 time steps and temperatures calculated using the finite element model, extracted at several positions vertical to the probes location. The calculated temperature fields are shown for the 1st August 2016 (b) and the 1st November 2016 (c). This highlight the temperature wave front and the surface temperature variations imposed at boundary conditions for the finite element modelling. The boundary between upper and lower layers is highlighted in (b) and (c) as well as the position of the temperature probes.**

## References

- Brunet, P., Clément, R. and Bouvier, C.: Monitoring soil water content and deficit using Electrical Resistivity Tomography (ERT) – A case study in the Cevennes area, France, *J. Hydrol.*, 380(1–2), 146–153, doi:10.1016/j.jhydrol.2009.10.032, 2010.
- Chambers, J. E., Gunn, D. A., Wilkinson, P. B., Meldrum, P. I., Haslam, E., Holyoake, S., Kirkham, M., Kuras, O., Merritt, A. and Wragg, J.: 4D electrical resistivity tomography monitoring of soil moisture dynamics in an operational railway embankment, *Surf. Geophys.*, 12(2007), doi:10.3997/1873-0604.2013002, 2014.
- Clauser, C. and Huenges, E.: Thermal conductivity of rocks and minerals, *Rock Phys. Phase Relat. Handb. Phys. Constants*, 105–126, 1995.
- Farouki, O. T.: Thermal properties of soils, Cold Regions Research and Engineering Lab Hanover NH., 1981.
- Günther, T., Rücker, C. and Spitzer, K.: Three-dimensional modelling and inversion of dc resistivity data incorporating topography - II. Inversion, *Geophys. J. Int.*, 166(2), 506–517, doi:10.1111/j.1365-246X.2006.03011.x, 2006.
- Hayley, K., Bentley, L. R., Gharibi, M. and Nightingale, M.: Low temperature dependence of electrical resistivity: Implications for near surface geophysical monitoring, *Geophys. Res. Lett.*, 34(18), L18402, doi:10.1029/2007GL031124, 2007.
- Keller, G. V. and Frischknecht, F. C.: Electrical methods in geophysical prospecting, 1966.
- Rücker, C., Günther, T. and Spitzer, K.: Three-dimensional modelling and inversion of dc resistivity data incorporating topography - I. Modelling, *Geophys. J. Int.*, 166(2), 495–505, doi:10.1111/j.1365-246X.2006.03010.x, 2006.
- Rücker, C., Günther, T. and Wagner, F.: PyGIMLi - An Open Source Python Library for Inversion and Modelling in Geophysics., 2016.
- Rücker, C., Günther, T. and Wagner, F. M.: pyGIMLi: An open-source library for modelling and inversion in geophysics, *Comput. Geosci.*, doi:10.1016/j.cageo.2017.07.011, 2017.
- Samouëlian, A., Cousin, I., Tabbagh, A., Bruand, A. and Richard, G.: Electrical resistivity survey in soil science: a review, *Soil Tillage Res.*, 83(2), 173–193, doi:10.1016/j.still.2004.10.004, 2005.
- Trombe, F.: *Traité de spéléologie*, Payot Paris., 1952.
- Uhlemann, S., Smith, A., Chambers, J., Dixon, N., Dijkstra, T., Haslam, E., Meldrum, P., Merritt, A., Gunn, D. and Mackay, J.: Assessment of ground-based monitoring techniques applied to landslide investigations, *Geomorphology*, 253, 438–451, doi:10.1016/j.geomorph.2015.10.027, 2016.
- Vosteen, H.-D. and Schellschmidt, R.: Influence of temperature on thermal conductivity, thermal capacity and thermal diffusivity for different types of rock, *Phys. Chem. Earth Parts ABC*, 28(9), 499–509, 2003.